Phenol-Glyoxal Precondensate Crosslinked Soy Protein Adhesive and Its Plywood Manufacturing Process

Jiankun Liang,[a,#] Yuqi Yang,[b,#] Qiuli Li,[b] Ningyuan Zuo,[b] Chuchu Chen,[b] Tong Meng,[b] Huali Li,[b] Zhixian Song,[b] Caihong Long,[b] Yulan Jian,[a,*] and Zhigang Wu,[b,*]

To develop high-performance soy protein-based adhesives, this study employed a phenol-glyoxal precondensate as a crosslinking agent and optimized the hot-pressing process parameters for plywood through orthogonal experiments, exploring its feasibility for application in wood-based panel manufacturing. Electrospray ionization mass spectrometry (ESI-MS) and nuclear magnetic resonance (^{13}C-NMR) analyses revealed the self-polymerization behavior of glyoxal and its condensation reaction pathway with phenol under acidic conditions, confirming that cyclic ether intermediates were predominant. Using boiling water-resistant bond strength as the evaluation index, orthogonal experiments were conducted to optimize hot-pressing temperature, pressure, time, and glue spread amount. The results demonstrated that hot-pressing temperature exerted the greatest influence on performance, with the optimal conditions being 170 °C, 1.4 MPa, 1.0 min/mm, and 330 g/m^2. The crosslinking agent enhanced the compactness and water resistance of the adhesive layer through multi-site covalent bonding, hydrogen bond entanglement, and π-π stacking, providing a reference for the industrial application of bio-based adhesives.

DOI: 10.15376/biores.21.2.4135-4152

Keywords: Soy protein adhesive; Phenol-glyoxal precondensate; ESI-MS; ^{13}C-NMR; Orthogonal experiment; Plywood

*Contact information: a: College of Civil Engineering, Kaili University, Qiandongnan 556011, China; b: College of Forestry, Guizhou University, Guiyang 550025, China; #: These two authors contributed equally to this work; *Corresponding authors: Jianyulan1992@163.com; wzhigang9@163.com*

INTRODUCTION

Driven by increasingly stringent environmental regulations worldwide and the accelerating transition toward sustainable development, the wood-based panel industry is currently undergoing a pivotal shift away from conventional petroleum-based adhesives toward environmentally friendly bio-based alternatives. The selection and design of crosslinking agents play a decisive role in enhancing the water-resistant bonding performance of bio-based adhesives, as they effectively overcome the inherent hydrophilic defects of natural macromolecules by constructing dense three-dimensional network structures (Liu *et al*. 2022; Westerman *et al*. 2023; Xu *et al*. 2023; Yang *et al*. 2023; Lin *et al*. 2024; Zeng *et al*. 2024; Li *et al*. 2025a, 2025b; Zhou *et al*. 2025). Soy protein has emerged as one of the most promising adhesive base materials due to its renewable source, low cost, and abundance of reactive functional groups such as amino and carboxyl moieties. However, early soy protein adhesives suffered from critical limitations including poor water resistance, insufficient bonding strength, and susceptibility to mildew, which severely restricted their industrial application (Zhang *et al*. 2022a; Hou *et al*. 2025; Zheng

et al. 2025). In recent years, researchers have significantly improved their performance through chemical modification, nano-reinforcement, and efficient crosslinking, particularly by employing crosslinking agents, such as epoxy resins and isocyanates, to substantially enhance water resistance (Pang *et al*. 2022; Bai *et al*. 2023; Jiang *et al*. 2025; Yao *et al*. 2025).

Phenol-formaldehyde resin, due to the strong reactivity of hydroxymethyl functional groups on its benzene rings, can form dense crosslinked network structures with functional groups in protein molecular chains—including amino, amide, carboxyl, and hydroxyl moieties—through multiple mechanisms, such as condensation reactions and nucleophilic addition, thereby enhancing adhesive bonding strength, water/weather resistance, and thermal stability. This modification strategy has been validated in numerous studies (Yang *et al*. 2006; Lei *et al*. 2016; Wu *et al*. 2019; Xu *et al*. 2020). However, conventional phenolic resin synthesis typically suffers from high residual levels of free formaldehyde and free phenol, which not only leads to continuous VOC emissions during adhesive use—a hazard to both the production environment and human health—but also constrains large-scale application in fields with stringent environmental requirements, such as modern home furnishings and prefabricated buildings.

To address these issues, the authors previously leveraged glutaraldehyde's two highly reactive aldehyde groups by incorporating it into the phenolic resin synthesis system. This system can rapidly form dynamic, reversible Schiff base structures with protein side-chain amino groups and further construct stable covalent crosslinking networks through subsequent reactions. This modification strategy not only effectively improved the bonding strength of soy protein adhesives and reduced free phenol/aldehyde content, but it also endowed the adhesive with anti-degradation properties due to glutaraldehyde's inherent antibacterial characteristics (Wu *et al*. 2017). Nevertheless, the glutaraldehyde modification system exhibits certain limitations, including susceptibility to aldol condensation self-polymerization during storage, resulting in excessively rapid viscosity increase and shortened pot life, as well as high raw material costs and strong pungent odor—factors unfavorable for long-term industrial promotion.

Glyoxal, which comprises just two carbon atoms, represents the simplest saturated dialdehyde. It has garnered significant attention in recent years, serving dual roles as an industrial raw material and an effective crosslinking agent. This multifunctional aldehyde compound is distinctly characterized by an exceptional combination of high chemical reactivity, notably low toxicological profile, and outstanding cost-effectiveness relative to alternative agents. Extensive research investigations have systematically demonstrated that glyoxal possesses numerous practical advantages, including superior chemical reactivity that facilitates efficient processing, effective antimicrobial sterilization capabilities, minimal physiological irritation potential, weak corrosive properties toward equipment and substrates, economically favorable production costs, excellent water solubility for aqueous formulation compatibility, and remarkably broad applicability across diverse industrial sectors. In direct comparative toxicological assessments against formaldehyde, a widely used but hazardous crosslinking agent, glyoxal exhibits approximately two hundred-fold lower volatility characteristics and demonstrates a sixty percent reduction in acute toxicity metrics, while completely eliminating the definitive carcinogenic risks associated with formaldehyde exposure. Consequently, these favorable safety and performance attributes establish glyoxal as an inherently safer crosslinking agent suitable for sustainable industrial applications. Its two adjacent aldehyde groups maintain high reactivity while the shortened carbon chain significantly reduces molecular escape tendency and biological damage

effects (Wu *et al*. 2021; Rodriguez *et al*. 2022; Chen *et al*. 2023; Hsu *et al*. 2024). Relative to glutaraldehyde, glyoxal's molecular weight is merely one-third, achieving a 2.5-fold increase in reaction efficiency per unit mass—a structural advantage attributable to its higher functional group density and lower steric hindrance (Yamamoto *et al*. 2020; Park *et al*. 2023; Müller *et al*. 2024). Critically, unlike glutaraldehyde, which invariably contains unavoidable enal irritant impurities as inherent byproducts of its manufacturing process, glyoxal is completely free from such deleterious contaminants, thereby offering a substantially milder odor profile, significantly enhanced operational environment friendliness for industrial personnel, and remarkably superior storage stability characterized by minimal autopolymerization deterioration during extended shelf life. Currently, glyoxal is demonstrating exceptional application potential across diverse industrial and scientific fields, specifically encompassing textile finishing processes, paper reinforcement technologies, biological tissue crosslinking applications, and pharmaceutical intermediate synthesis procedures, thereby comprehensively leveraging its multifaceted advantages of being simultaneously efficient in chemical reactivity, low in toxicological hazard, economical in production costs, and environmentally benign in ecological impact.

To develop high-performance soy protein-based adhesives, this study employs a phenol-glyoxal precondensate as the crosslinking agent to optimize plywood hot-pressing process parameters through orthogonal experiments and investigate its application feasibility in wood-based panel manufacturing. Compared with conventional phenol-formaldehyde resins, the phenol-glyoxal crosslinking system exhibits significant advantages in environmental compliance, reaction controllability, and process adaptability. This system completely eliminates formaldehyde usage and possesses industrialization potential due to widely available raw materials and low cost. Moreover, the precondensate is rich in hydroxyl groups, ether bonds, and residual aldehyde groups, enabling multiple crosslinking interactions—including hydrogen bonding and covalent bonding—with protein macromolecules. The resulting network structure demonstrates superior balance between compactness and toughness compared to linear phenolic resins, providing an innovative technical pathway for developing green high-performance soy protein-based adhesives.

EXPERIMENTAL

Materials

Soy protein isolate (protein content 90%) was purchased from Shandong Gushen Biological Technology Group Co., Ltd. Phenol (99 wt%) and glyoxal (40 wt%), both analytical grade, were obtained from Sinopharm Chemical Reagent Co., Ltd. Poplar veneer (*Populus* spp., moisture content 8 to 10%) with dimensions of 400 mm × 400 mm and a thickness of 1.5 mm was purchased from Shuyang, Jiangsu, China.

Preparation of Phenol-Glyoxal Precondensate

In a three-necked round-bottom flask equipped with a mechanical stirrer, thermometer, and reflux condenser, phenol (28.2 g) was added. The pH was adjusted to 1.0 using oxalic acid, and the mixture was heated to reflux and maintained (ca. 0.5 h). With constant stirring, glyoxal solution (36.25 g) was slowly added dropwise *via* a constant-pressure dropping funnel at a rate of 6 drops per minute (*ca.* 1.5 h). After the addition was

complete, the reaction was continued at reflux for 3.5 h. Upon completion of the reaction, the mixture was cooled to room temperature and discharged.

Preparation of Soy Protein Adhesive and Plywood

The soy protein adhesive (Wu *et al*. 2025) was uniformly blended with the phenol-glyoxal precondensate crosslinker at a fixed addition level of 15 wt% based on SPI solids (dry weight basis); trace ammonia water was introduced to prevent excessively rapid crosslinking during mixing. The components were mechanically blended for 5 min, and then the resulting adhesive was directly used for plywood fabrication. The adhesive was applied to the veneer surfaces using a hand brush to ensure uniform coverage. The solid content and viscosity of the adhesive were determined according to the standard GB/T 14074 (2017). Three-layer poplar plywood (400 mm × 400 mm) was fabricated in the laboratory. Using hot-pressing temperature, pressure, time, and glue spread amount as the four experimental factors, with boiling water-resistant bond strength as the evaluation index, the experiments were designed according to the orthogonal array L16 (4^4) (Table 1). The final boiling water-resistant strength was reported as the average of 12 specimens.

Table 1. Orthogonal Experiment Design Formulation of Plywood

Levels	Factors			
	Hot-Pressing Temperature (°C)	Hot-Pressing Pressure (MPa)	Hot-Pressing Time (min/mm)	Adhesive Consumption (g/m^2)
1	140	1.0	1.0	290
2	155	1.2	1.2	310
3	170	1.4	1.4	330
4	185	1.6	1.6	350

Electrospray Ionization Mass Spectrometry (ESI-MS) Testing

The samples for ESI-MS analysis were lyophilized (freeze-dried) and then dissolved in chloroform (10 μL/mL). The samples were dissolved in chloroform to prepare a solution at a concentration of 10 μL/mL (10 μL sample in 1 mL chloroform) and directly infused into a Waters Xevo TQ-S mass spectrometer *via* electrospray ionization at a flow rate of 5 μg/s. Spectra were acquired in positive ion mode with an ion energy of 0.3 eV.

Nuclear Magnetic Resonance (^{13}C-NMR) Testing

Samples for 13C-NMR analysis were prepared by mixing 300 μL of the liquid sample with 100 μL of dimethyl sulfoxide-d6 (DMSO-d6). ^{13}C-NMR (zgig) spectra were recorded on a Bruker Avance 600 MHz spectrometer using inverse-gated proton decoupling to achieve adequate signal-to-noise ratio. All analyses were conducted with a relaxation delay of 6 s, and chemical shifts were accurate to within 1 ppm.

Statistical Analysis

The data were processed using Excel 2021 and Origin 2024 software, and the significance of differences was judged *via* the one-way analysis of variance (ANOVA) ($p < O.05$). The error bars represent standard deviation.

RESULTS AND DISCUSSION

ESI-MS Analysis

This study characterized the molecular distribution features of glyoxal and phenol-glyoxal precondensate using positive-ion mode ESI-MS, with the results shown in Figs. 1 and 2, respectively. Due to the facile formation of Na^+ adducts during ionization, the observed mass-to-charge ratios required subtraction of the sodium ion mass (23 Da) to obtain the actual molecular weights of neutral species. Table 2 summarizes the possible structural assignments for the major characteristic peaks.

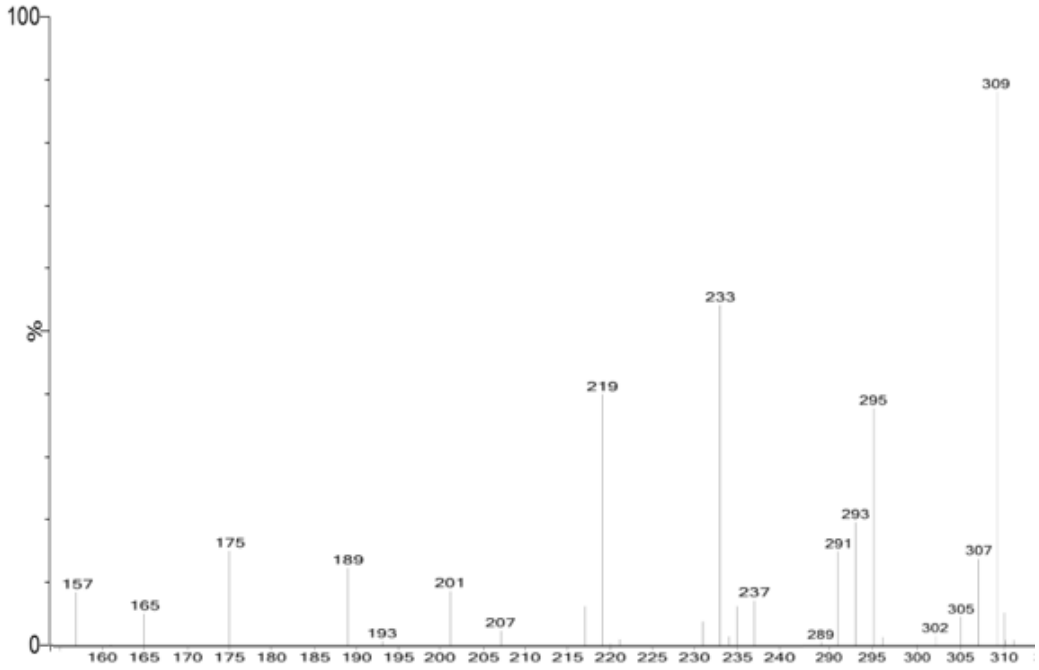

Fig. 1. ESI-MS spectrum of glyoxal under acidic conditions

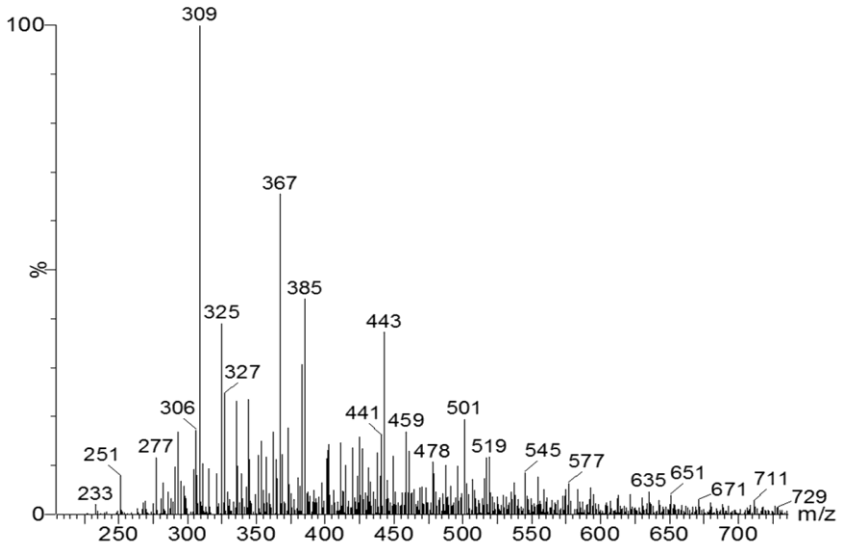

Fig. 2. ESI-MS spectrum of phenol-glyoxal precondensate

Table 2. Orthogonal Experiment Design Formulation of Plywood ESI-MS Analysis of Glyoxal and Phenol-glyoxal Precondensation and Main Structural Assignment

Experimental $[M+Na]^+$ (Da)	Structures	Source
175	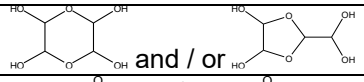	Glyoxal
201	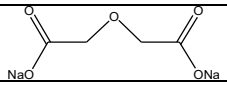	Glyoxal
219	2 CH_2OH-COONa	Glyoxal
233	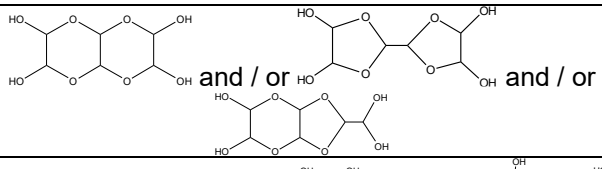	Glyoxal
251	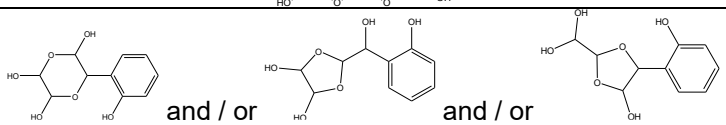	phenol-glyoxal
291	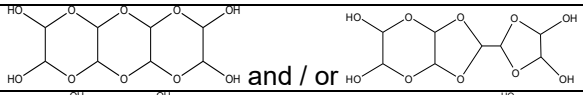	Glyoxal
327	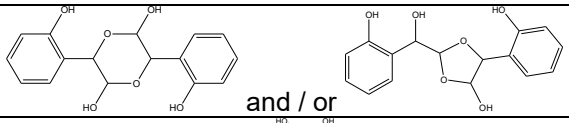	phenol-glyoxal
309	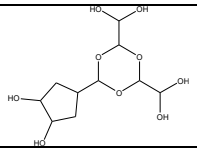	Glyoxal
385	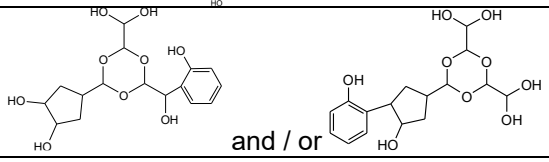	Glyoxal

The mass at 219 Da corresponds to sodium glycolate, whose formation can be traced to the disproportionation of glyoxal under acidic catalysis—wherein two glyoxal molecules undergo an intramolecular redox reaction to generate one glycolic acid molecule. This product subsequently forms a stable salt-type adduct with Na^+ and is thus detected. The peak at 201 Da differs from 219 Da by 18 Da, precisely matching the mass loss of one water molecule, which arises from esterification between two glycolic acid molecules and further corroborates the occurrence of disproportionation. In acidic aqueous systems, glyoxal readily undergoes hydration to form glyoxal tetrol due to the absence of α-hydrogens; however, this intermediate exhibits extremely poor thermodynamic stability and cannot exist in isolation. To minimize system energy, glyoxal tetrol undergoes intramolecular cyclic etherification to form stable cyclic oligomers. Among these, the signal at 175 Da likely corresponds to a monomeric cyclic ether structure with either five- or six-membered rings. As the degree of polymerization increases, peaks at 233, 291, and 309 Da are sequentially assigned to cyclic oligomers of varying condensation degrees. The 309 Da species exhibits the highest abundance, indicating that glyoxal predominantly exists as a specific cyclic configuration under acidic conditions—consistent with ring strain

theory, where five- and six-membered rings become favored conformations due to minimal bond angle distortion (Wu *et al*. 2021).

The condensation reaction in the phenol-glyoxal system demonstrates significant structural polymorphism. The 251 Da species is attributed to mono-condensation products of phenol and glyoxal, which may exist as three constitutional isomers: ortho-ortho bridging, ortho-para bridging, or para-para linkage. Similarly, the 385 Da peak also represents a mono-condensation product, but it exists in only two major configurations due to further cyclization or substituent arrangement differences. The signal at 327 Da clearly corresponds to di-condensation products, representing oligomeric structures formed by two phenol units bridged by glyoxal, which likewise exist as two positional isomers.

These results demonstrate that glyoxal exhibits multiple competing reaction pathways under acidic conditions: the intramolecular cyclic etherification route generates stable self-polymerized species, whereas phenol co-condensation dominates when phenol is present. The product distribution is jointly regulated by reaction kinetics and thermodynamic stability.

^{13}C-NMR Analysis

Building on the limitations of the ESI-MS analysis regarding sodium ion adduct formation and isomeric overlap, ^{13}C-NMR provides more precise structural group identification capabilities. The characteristic chemical shifts of carbon atoms in different chemical environments effectively reveal the microstructure of the molecular skeleton; the results are shown in Figs. 3 and 4. The series of signals at chemical shifts of 91.62, 93.02, 95.77, and 98.88 ppm are unambiguously assigned to five- and six-membered cyclic ether structures formed by intramolecular cycloetherification of glyoxal. Their chemical shift range closely matches the characteristics of acetal carbons, confirming the existence of cyclic oligomers, such as the 175 Da species, in Table 2.

Multiple sets of new signals at 70.01, 92.05, 93.86, 94.93, 96.75, and 100.65 ppm indicate a reaction between phenol and cyclic ether glyoxal. Particularly, the downfield shift at 100.65 ppm reflects enhanced electron-withdrawing effects of the acetal carbon directly attached to the aromatic ring, which mutually validates the formation mechanism of phenol-glyoxal adducts, such as those at 251 and 327 Da, observed in ESI-MS. Through integrating molecular weight information from mass spectrometry and carbon skeletal fingerprints from NMR, a complete competitive reaction network under acidic conditions can be delineated (Fig. 5). This pathway comprises: (1) rapid hydration-cyclization equilibrium of glyoxal to form thermodynamically stable cyclic structures; (2) Cannizzaro-type disproportionation between two molecules to generate glycolate (Wu *et al.* 2021); (3) phenol preferentially capturing the cyclic ether active intermediates *via* ortho/para electrophilic substitution to produce the 251 Da mono-condensation product, which undergoes further secondary substitution to form the 327 Da di-condensation oligomer. The NMR data excludes the possibility of linear oligomers, confirming cyclic ether structures as the overwhelmingly dominant intermediates.

Using the phenol-glyoxal precondensate as a crosslinking agent, its cyclic/open-ring hybrid structure rich in hydroxyl groups, ether bonds, and residual aldehyde groups, can undergo multi-site cooperative reactions with soy protein polypeptide chains. Residual aldehyde groups react with protein amino groups *via* Schiff base formation, which subsequently stabilize into covalent crosslinks (Wu *et al*. 2021; Hsu *et al*. 2024), while carboxyl and hydroxyl groups form covalent bonds through esterification with aspartic/glutamic acid residues, thereby achieving irreversible bridging of protein chain

segments (Lei *et al*. 2016; Wu *et al*. 2019). The C-O-C bond angle of the rigid cyclic ether skeleton exhibits high geometric compatibility with the hydrogen bond donor/acceptor geometry of protein amide bonds, enabling topological entanglement through multi-site hydrogen bonding (O-H···O=C-N) and significantly enhancing network compactness (Wu *et al*. 2025). Additionally, the introduced benzene ring structure provides both π-π stacking interactions with aromatic amino acid residues (tyrosine, phenylalanine) (Zhang *et al*. 2022b; Yang *et al*. 2023) and steric hindrance effects, effectively shielding crosslinking nodes, inhibiting water-induced swelling, while simultaneously avoiding the excessive rigidity of conventional phenolic resins. Furthermore, upon thermal activation during hot-pressing (≥170°C), the cyclic acetal structures undergo thermally induced ring-opening reactions, exposing secondary hydroxyl groups that form additional ester bonds with protein carboxyl groups (Yamamoto *et al*. 2020; Chen *et al*. 2023), thereby driving the evolution of crosslinking nodes from single chemical bonding toward a dual chemical-physical network architecture.

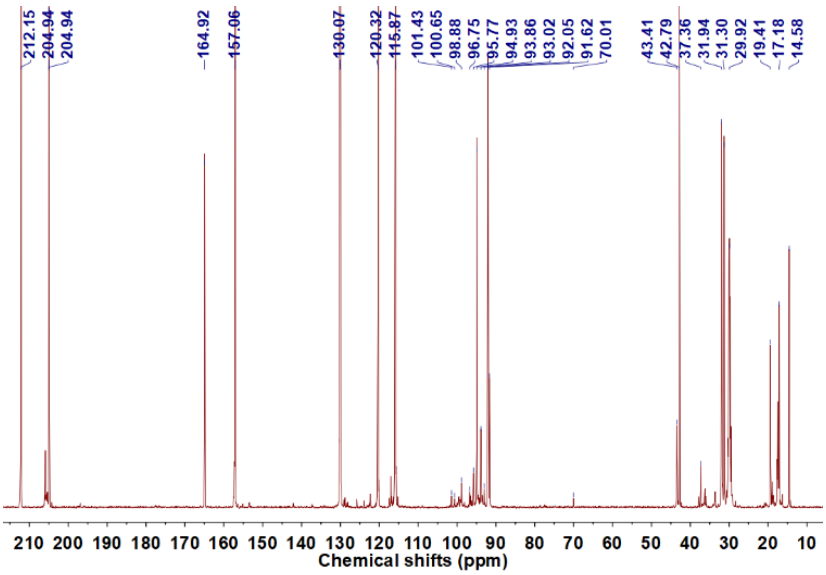

Fig. 3. 13C-NMR spectrum of phenol-glyoxal precondensate

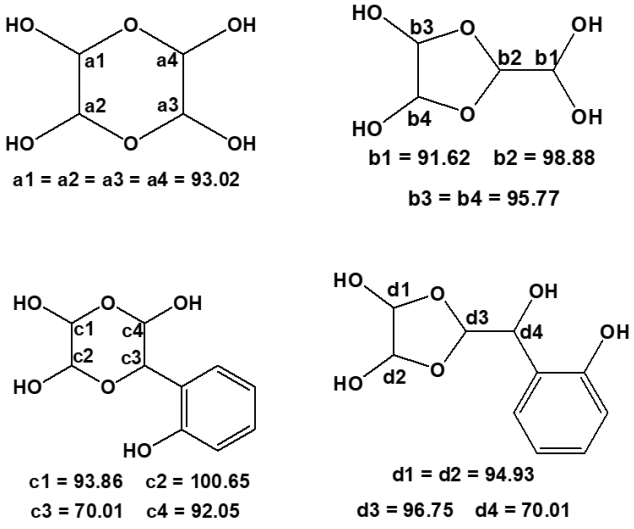

Fig. 4. Main structural and chemical shift patterns of the phenol-glyoxal precondensate

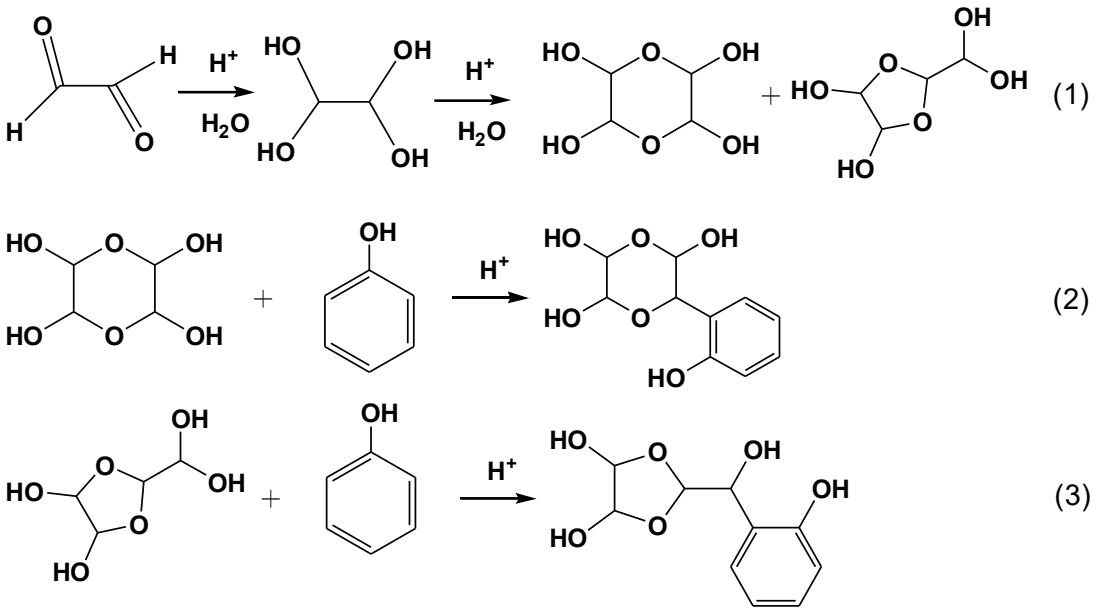

Fig. 5. Reaction pathway of the phenol-glyoxal precondensate

Orthogonal Test Results and Analysis

Prior preliminary experiments demonstrated that the pristine SPI adhesive inherently failed to meet boiling water tolerance requirements even without any modification. Consequently, this orthogonal study was deliberately confined to the phenol-glyoxal crosslinked system as a targeted process optimization. Tables 3 and 4 reveal the influence patterns of hot-pressing process parameters on the boiling water-resistant bond strength of plywood bonded with phenol-glyoxal crosslinked soy protein adhesive. Both range analysis and variance analysis consistently demonstrate that hot-pressing temperature exhibits overwhelming dominance over bonding performance, with the effect hierarchy following: hot-pressing temperature >> hot-pressing pressure > hot-pressing time = glue spread amount. This ranking highlights the strong dependence of crosslinking reaction activation energy barriers on temperature, rather than relying solely on pressure-driven rheological penetration or time accumulation effects.

Consistent with its role as a key diagnostic indicator, the wood failure rate increased in tandem with bond strength as the temperature rose, validating the temperature-driven improvement in bonding performance. For the 140 °C series, wood failure rates below 10% indicate that the dominant failure modes were cohesive failure within the adhesive layer or interfacial adhesion failure, reflecting a fragile crosslinked network. The 155 °C series showed increased wood failure rates of 10 to 16%, suggesting enhanced wood-adhesive interfacial interactions, yet still failing to achieve a failure mode transition. When temperature was greater than or equal to 170 °C, wood failure rates jumped to 45 to 53%, marking a shift toward substrate wood tearing. The 185 °C series further achieved high wood failure rates of 76 to 83%, demonstrating that the bonding system not only met strength requirements but also had excellent toughness and energy dissipation capacity, with the adhesive layer forming deep mechanical interlocking and chemical bonding with wood microstructures, such as vessels and fibers, thereby approaching an ideal state of bonding reliability.

Table 3. Range Analysis of Orthogonal Experiment Results

No.	Hot-Pressing Temperature (°C)	Hot-Pressing Pressure (MPa)	Hot-Pressing Time (min/mm)	Adhesive Consumption (g/m^2)	Shear Strength (MPa)	Wood Failure Rate (%)
1	140	1.0	1.0	290	0.40±0.02	5
2	140	1.2	1.2	310	0.48±0.02	0
3	140	1.4	1.4	330	0.57±0.03	8
4	140	1.6	1.6	350	0.53±0.02	0
5	155	1.0	1.2	330	0.65±0.03	16
6	155	1.2	1.0	350	0.65±0.04	12
7	155	1.4	1.6	290	0.73±0.04	10
8	155	1.6	1.4	310	0.71±0.03	10
9	170	1.0	1.4	350	0.72±0.04	45
10	170	1.2	1.6	330	0.74±0.05	51
11	170	1.4	1.0	310	0.85±0.06	53
12	170	1.6	1.2	290	0.85±0.04	48
13	185	1.0	1.6	310	0.84±0.05	83
14	185	1.2	1.4	290	0.91±0.05	76
15	185	1.4	1.2	350	0.86±0.04	84
16	185	1.6	1.0	330	0.90±0.06	80
Shear Strength in Boiling Water (MPa)						
K1	0.495	0.652	0.723	0.677	—	—
K2	0.685	0.695	0.720	0.708	—	—
K3	0.790	0.752	0.715	0.727	—	—
K4	0.877	0.747	0.690	0.735	—	—
R	0.382	0.100	0.033	0.058	—	—

Note: K1, K2, K3, and K4, respectively, represent the sum of the indicators of this factor at level 1 (hot-pressing temperature), level 2 (hot-pressing pressure), level 3 (hot-pressing time), and level 4 (adhesive consumption); R stands for range.

Table 4. Variance Analysis of Orthogonal Experiment on Bonding Strength in Boiling Water

Factors	Sum of squares	df	Mean square	F value	Significance
Hot-pressing temperature (°C)	0.325	3	0.108	130.000	**
Hot-pressing pressure (MPa)	0.027	3	0.009	10.800	*
Hot-pressing time (min/mm)	0.002	3	0.001	0.800	—
Adhesive consumption (g/m^2)	0.003	3	0.001	1.200	—
Error	0.010	6	0.002	—	—

Effect of Hot-pressing Temperature on Bonding Strength of Plywood

Figure 6 illustrates the influence of hot-pressing temperature on the boiling water-resistant bond strength of plywood bonded with phenol-glyoxal precondensate crosslinked soy protein adhesive. Experimental data demonstrated a typical nonlinear growth trend in

bond strength with increasing temperature: 0.495 MPa at 140 °C, surging to 0.685 MPa at 155 °C (a 38.4% increase), further rising to 0.790 MPa at 170 °C, and reaching 0.877 MPa at 185 °C. Notably, the rate of strength enhancement gradually decelerated with temperature, with a marked reduction in gain after 170 °C, implying that the crosslinking reaction approached a saturation critical point within this temperature domain. The bond strength threshold (≥ 0.70 MPa) was first exceeded at 155 °C, yet this borderline condition proved unreliable. In contrast, 170 and 185 °C surpassed the threshold 13% and 25%, respectively, confirming that only temperatures of 170 °C and above ensured stable, compliant bonding performance.

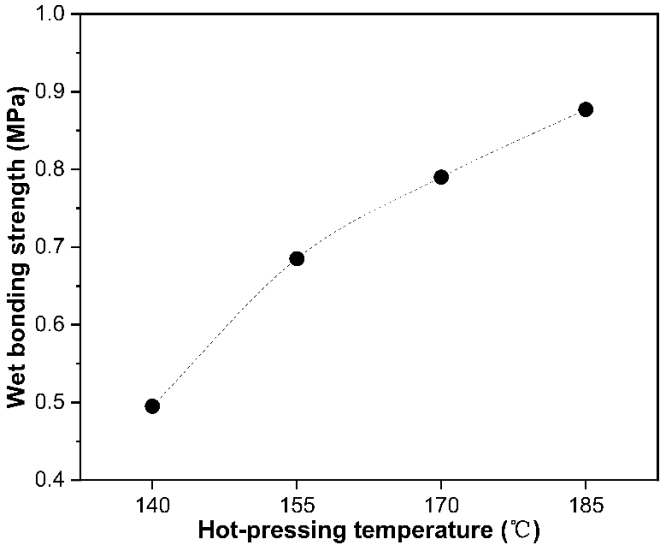

Fig. 6. Effect of hot-pressing temperature on bonding strength of plywood

The increase in hot-pressing temperature favored the bonding system through multiple synergistic mechanisms. First, elevated temperature significantly reduced adhesive viscosity, enhancing wetting, spreading, and penetration on wood surfaces. This promoted thorough diffusion of the adhesive into microscopic pores, such as cell lumens and vessels, forming tighter mechanical interlocking and interfacial engagement (Wu *et al*. 2025). Second, increasing the temperature from 140 to 170 °C activated the system and accelerated polycondensation, facilitating complete and uniform curing that yielded a dense, well-developed network structure in the adhesive layer. Third, the cyclic ether structures in the precondensate underwent thermally induced ring-opening reactions, exposing secondary hydroxyl groups that can form additional ester bonds with protein carboxyl groups (Liang *et al*. 2026). This "thermally activated" effect drives the evolution of crosslinking nodes from single chemical bonding toward a dual "chemical-physical" network architecture, thus further enhancing system compactness and stability.

Concurrently, the temperature field's activation of wood components constitutes another dimension of "adhesive-wood" synergistic enhancement. Hemicellulose begins deacetylation above 160 °C, generating furfural derivatives that undergo secondary condensation with hydroxymethyl groups in the precondensate to construct supplementary crosslinks (Wu *et al*. 2025). When temperature exceeds the lignin glass transition temperature (Setter *et al.* 2021; Tene Tayo *et al.* 2025; Zhou *et al.* 2025), its three-dimensional network softens and melts, thereby enabling molecular chain rearrangement and interfacial entanglement under pressure that noticeably strengthens mechanical

interlocking. However, excessively high temperatures introduce considerable drawbacks: wood surfaces develop scorched brown discoloration from pyrolysis, degrading appearance quality; energy consumption rises substantially, increasing production costs; and wood compression rates increase markedly, reducing raw material utilization. In comparison, 170 °C not only achieves an optimal trade-off between strength and cost but, more critically, maintains a balanced controllability and toughness of the crosslinked network. Therefore, comprehensive performance establish 170 °C as the most suitable hot-pressing temperature.

Effect of Hot-pressing Pressure on Bonding Strength of Plywood

Figure 7 illustrates the influence of hot-pressing pressure on the boiling water-resistant bond strength of plywood bonded with phenol-glyoxal precondensate crosslinked soy protein adhesive. When pressure increased from 1.0 to 1.2 MPa, bond strength increased 6.6% to 0.695 MPa. Further increasing to 1.4 MPa expanded this increment to 8.2%, indicating a reinforcing effect on interfacial bonding at this stage. However, when pressure was raised beyond to 1.6 MPa, strength declined to 0.747 MPa, which, although not falling below the 1.2 MPa level, already showed signs of diminishing returns.

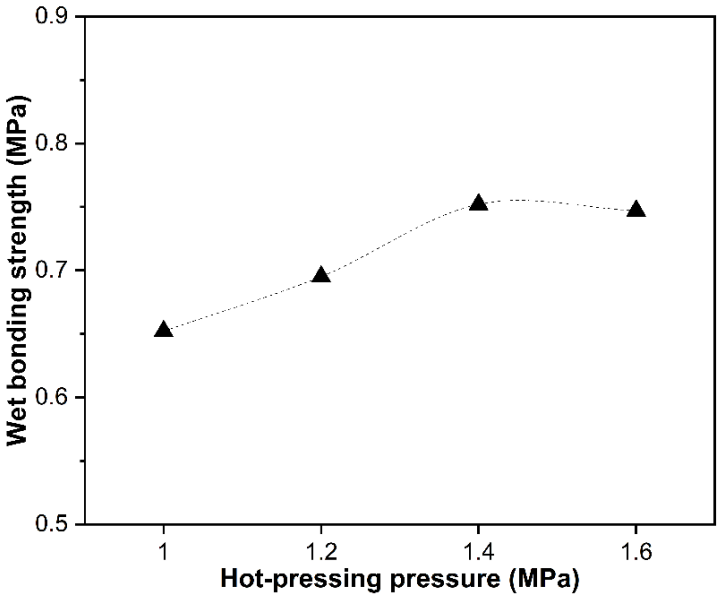

Fig. 7. Effect of hot-pressing pressure on bonding strength of plywood

At the macroscopic level, applying pressure primarily drives the high-viscosity soy protein adhesive to overcome surface energy barriers, achieving mechanical interlocking and molecular-level contact with the rough veneer surface. At the mesoscopic level, moderate pressure (1.2 to 1.4 MPa) induces shear-thinning of the adhesive, improving its penetration and spreading within fiber vessels and cell lumens, and promoting uniform formation of "adhesive nail" structures. Yet, when pressure exceeds the critical threshold (> 1.4 MPa), hydrostatic pressure within the adhesive layer surges, forcing uncured resin to migrate toward edges and squeeze out, thereby creating local "glue-starved" defects. Simultaneously, excessive compressive stress may crush the fragile thin-walled cells on the wood surface, reducing mechanical interlocking efficiency and ultimately weakening bond strength.

For the phenol-glyoxal precondensate crosslinked soy protein adhesive system, its noticeable thickening effect necessitates pressure sufficient to disrupt air entrapment at the adhesive–wood interface, yet it is important to avoid adhesive loss from over-compaction. Therefore, 1.4 MPa represents the optimal hot-pressing pressure, reflecting the interplay between adhesive layer crosslinking/curing progression and spreading/penetration capability.

Effect of Hot-pressing Time on Bonding Strength of Plywood

Figure 8 illustrates the effect of hot-pressing time on the boiling water-resistant bond strength of plywood bonded with phenol-glyoxal precondensate crosslinked soy protein adhesive. Over the 1.0 to 1.6 min/mm range, bond strength exhibits a slight decreasing trend, peaking at 0.723 MPa at 1.0 min/mm. When time increases to 1.2, 1.4, and 1.6 min/mm, strength declines modestly to 0.720, 0.715, and 0.690 MPa, respectively, with a maximum reduction of merely 4.6%, indicating insensitivity of bond strength to parameter variations within this interval. Nevertheless, 1.0 min/mm remained the optimal process setting for this system, at which point the soy protein adhesive curing reaction was substantially complete.

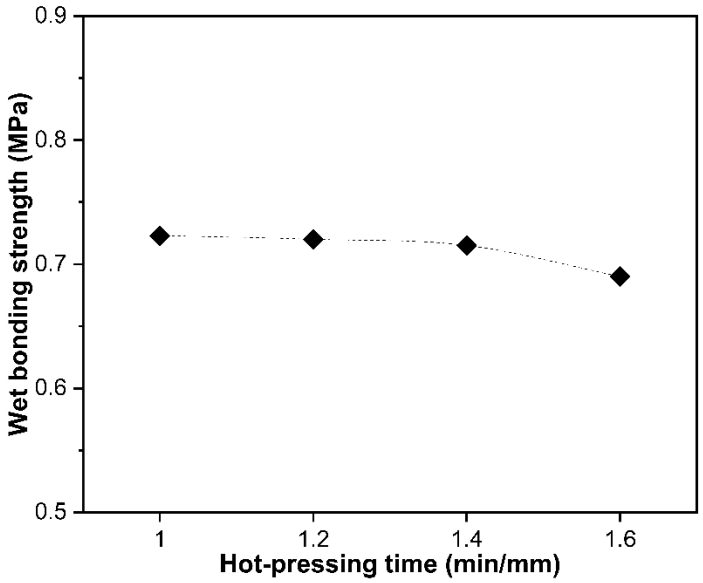

Fig. 8. Effect of hot-pressing time on bonding strength of plywood

For high-viscosity soy protein adhesive systems, the initial hot-pressing period ensures adequate wetting, capillary penetration, and mechanical interlocking between the adhesive and wood pore structures, while guaranteeing heat conduction from surface to interior to drive the crosslinking polycondensation reaction to completion. However, excessive hot-pressing time gives rise to multiple detrimental effects: first, over-crosslinking of the adhesive layer leads to increased three-dimensional network rigidity, reduced toughness, and heightened risk of internal stress concentration; second, prolonged high-temperature exposure may cause thermal degradation of adhesive functional groups and hydrolysis of wood hemicellulose, creating a weak boundary layer; third, extended production cycles significantly increase energy consumption and equipment occupancy costs (Wu *et al*. 2017, 2025). Notably, although the time parameter showed minimal impact, from an industrial production perspective, the 1.0 min/mm process window can

greatly reduce energy consumption and improve production efficiency while ensuring bonding performance, offering both technical feasibility and economic rationality. Therefore, a hot-pressing time of 1.0 min/mm is most appropriate.

Effect of Adhesive Consumption on Bonding Strength of Plywood

Figure 9 reveals the influence of glue spread amount (double-side**)** on the boiling water-resistant bond strength of plywood bonded with phenol-glyoxal precondensate crosslinked soy protein adhesive. Within the range of 290 to 350 g/m^2, bond strength exhibited a continuous upward trend. It reached 0.677 MPa at 290 g/m^2, increasing to 0.708 MPa at 310 g/m^2, further rising to 0.727 MPa at 330 g/m^2, and peaking at 0.735 MPa when the glue spread amount was increased to 350 g/m^2, representing an overall increase of 8.6%.

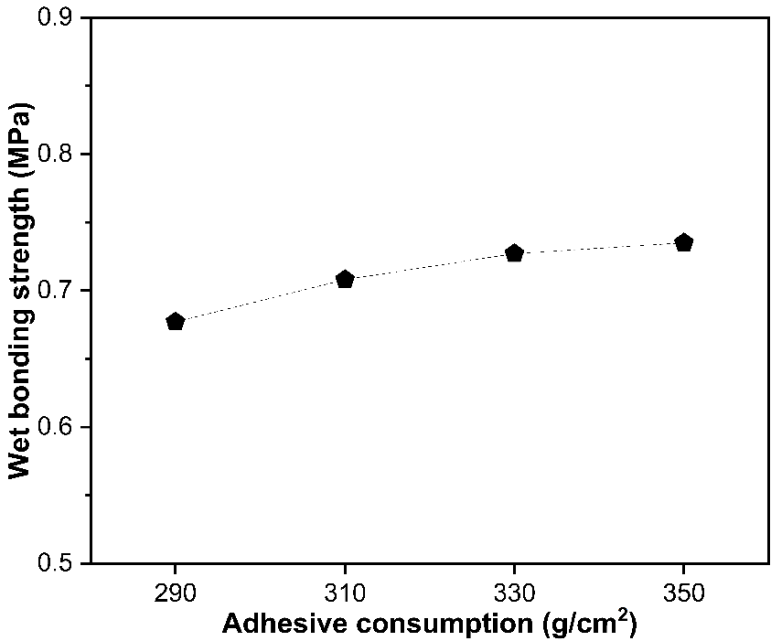

Fig. 9. Effect of adhesive consumption on bonding strength of plywood

From the perspective of bonding mechanism, the ideal adhesive layer should form a uniformly thick, continuous, and complete film on the wood surface. According to classical bonding theory, appropriately reducing adhesive layer thickness can be beneficial for bonding performance, as stress concentration effects within the layer intensify with increasing thickness (Hou *et al*. 2025; Li *et al*. 2025a). However, insufficient glue spread makes it difficult for the adhesive to adequately wet the wood surface, while restricted fluidity during hot-pressing prevents effective penetration, easily creating interfacial glue-starved defects that ultimately weaken the bond. Conversely, excessive glue spread also produces dual negative effects: first, during hot-pressing, the adhesive tends to overflow along channels, such as cell lumens, not only wasting material but also contaminating the press plates; second, an overly thick cured adhesive layer creates an imbalance between cohesive strength within the adhesive and adhesion at the wood-adhesive interface. When cohesive strength becomes the weak link, bond strength decreases rather than increases, while accumulated curing shrinkage stress also induces microcrack initiation in the cured layer.

Although variations in glue spread amount did not cause noticeable differences in bonding performance in this test, considering the requirements for process stability in industrial production and the rheological properties of the adhesive under hot-pressing conditions, 330 g/m^2 was determined as the optimal application parameter. This amount not only ensures adequate penetration of the adhesive into wood pore structures to form reliable mechanical interlocking and chemical bonding, but also avoids cost increases and internal stress deterioration caused by over-application, achieving a balance between performance and economy.

Since the theoretically optimal combination (170 °C, 1.4 MPa, 1.0 min/mm, 330 g/m^2) did not appear exactly among the 16 experimental runs of the orthogonal array L16(4^4), a confirmation test was conducted to validate the predicted optimal performance. Three replicate plywood panels were fabricated under the predicted optimal conditions and tested for boiling water–resistant bond strength according to GB/T 17657-2013. The results yielded a wet shear strength of 0.87 ± 0.03 MPa. The confirmation test verified that the orthogonal experimental design successfully identified the optimal hot-pressing parameters.

CONCLUSIONS

1. This study successfully developed a phenol-glyoxal precondensate crosslinked soy protein adhesive for plywood manufacturing, achieving excellent boiling water-resistant bonding strength under optimized hot-pressing conditions (170°C, 1.4 MPa, 1.0 min/mm, 330 g/m^2).
2. Through ESI-MS and ^{13}C-NMR characterization, the study elucidated that glyoxal forms stable cyclic ether intermediates under acidic conditions, which undergo ortho/para-substitution with phenol to create multi-site crosslinking architectures (combining covalent bonding, hydrogen bond entanglement, and π-π stacking). This mechanism enhances the adhesive layer's compactness, toughness, and water-swelling resistance compared to conventional linear phenolic systems.
3. Orthogonal experimental results demonstrated that hot-pressing temperature exerts the dominant influence on bonding performance, followed by pressure, while time and glue spread amount showed statistically insignificant effects within the tested ranges. Confirmation tests validated the reliability of the predicted optimal conditions.

ACKNOWLEDGMENTS

This work was supported by the Key Project of Basic Research of Guizhou Province of China (QKHJCZD[2026]021), Science-Technology Support Foundation of Qiandongnan of China ([2025]0009), Key Projects of Kaili University (2026ZD003), Science and Technology Achievement Project of Qiandongnan of China ([2024]2), and the Outstanding Youth Science and Technology Talent Project of Guizhou Province of China (YQK[2023]003).

REFERENCES CITED

Bai, M., Zhang, Y., Bian, Y., Gao, Q., Shi, Q.S., Cao, J., Zhang, Q., and Li, J. (2023). "A novel universal strategy for fabricating soybean protein adhesive with excellent adhesion and anti-mildew performances," *Chem. Eng. J.* 452, article 139359. https://doi.org/10.1016/j.cej.2022.139359

Chen, L., Wang, X., Zhang, Y., Liu, H., Wu, J., and Huang, M. (2023). "Glyoxal as a sustainable crosslinking agent for textile finishing: A comparative study with formaldehyde-based resins," *J. Clean. Prod.* 415, article 137892. https://doi.org/10.1016/j.jclepro.2023.137892

GB/T 14074 (2017). "Testing methods for wood adhesives and resins," Standardization Administration of China, Beijing, China.

Hou, M., Zhang, Q., Lei, H., Zhou, X., Du, G., Pizzi, A. Essawy, H., and Xi, X. (2025). "Mildew resistant modified starch adhesive by soybean meal flour crosslinking with excellent bonding properties," *Carbohyd. Polym.* 354, article 123247. https://doi.org/10.1016/j.carbpol.2025.123247

Hsu, C., Lim, S., Chen, Y., Wang, J., Tan, A., and Nakamura, H. (2024). "Glyoxal-crosslinked chitosan/gelatin hydrogel for sustained release of human platelet lysate to promote tissue regeneration," *Biomater. Sci.* 12(8), 2156-2170. https://doi.org/10.1039/D4BM00321A

Jiang, C., Robinson, B., Hu, J., and Wang, J. (2025). "Ambient pressure microwave-driven catalytic conversion of lignin to phenolic blend for soy protein adhesive application," *ACS Sustainable Chem. Eng.* 13, 13501-13507. https://doi.org/10.1021/acssuschemeng.5c05561

Lei, H., Wu, Z., Cao, M., and Du, G. (2016). "Study on the soy protein-based wood adhesive modified by hydroxymethyl phenol," *Polymers* 8(7), article 256. https://doi.org/10.3390/polym8070256

Li, C., Zhou, N., Guo, P., Li, M., Wang, F., Li, J., Han, Y., Wu, Z., and Lu, W. (2025b). "Innovative barnacle-inspired organic–inorganic hybrid magnesium oxychloride cement composites with exceptional mechanical strength and water resistance," *Adv. Compos. Hybrid Ma.* 8, article 43. https://doi.org/10.1007/s42114-024-01129-5

Li, D., Cai, B., Wang, Z., Jiang, Q., Ren, C., Wang, J., Wei, Z., Wu, Z, and Lei, H. (2025a). "Reducing curing temperature of multifunctional sucrose / tannic acid-based wood adhesive *via* catalysis method for improved water resistance and bonding strength," *Chem. Eng. J.* 525, article 170379. https://doi.org/10.1016/j.cej.2025.170379

Lin, Q., Ji, X., Sun, S., and Zhao, Z. (2024). "Breaking the barrier of high curing temperature: Efficient caramelization for fructose-based adhesives in a one-pot process," *ACS Sustainable Chem. Eng.* 12, 14128-14140. https://doi.org/10.1021/acssuschemeng.4c06228

Liu, Z., Liu, T., Gu, W., Zhang, X., Li, J., Shi, S. Q., and Gao, Q. (2022). "Hyperbranched catechol biomineralization for preparing super antibacterial and fire-resistant soybean protein adhesives with long-term adhesion," *Chem. Eng. J.* 449, article 137822. https://doi.org/10.1016/j.cej.2022.137822

Liang, J., Yang, Y.; Zuo, N., Li, Q., Song, Z., Long, C., Jian, Y., and Wu, Z. (2026). "Dual-pathway glyoxal–peptide reaction mechanisms under acidic and alkaline conditions for Camellia oleifera protein-based adhesive performance optimization," *BioResources* 21(1), 1207-1223. https://doi.org/10.15376/biores.21.1.1207-1223

Müller, B., Schmidt, A., and Li, C. (2024). "Glyoxal in pharmaceutical synthesis: High-efficiency intermediates for cephalosporin antibiotics and Vitamin A derivatives," *Org. Process Res. Dev.* 28(3), 1125-1138. https://doi.org/10.1021/acs.oprd.3c00456

Pang, H., Ma, C., and Zhang, S. (2022). "Conversion of soybean oil extraction wastes into high-performance wood adhesives based on mussel-inspired cation-π interactions," *Int. J. Biol. Macromol.* 209, 83-92. https://doi.org/10.1016/j.ijbiomac.2022.03.152

Park, J., Stevenson, D., and Martinez, F. (2023). "Molecular structure-reactivity relationship of short-chain dialdehydes: Why glyoxal outperforms glutaraldehyde in functional group density," *Green Chem. Lett. Rev.* 16(2), 189-201. https://doi.org/10.1080/17518253.2023.2189012

Rodriguez, P., Kumar, S., Anderson, R., and Thompson, K. (2022). "Toxicity profile assessment of dialdehyde crosslinkers: Glyoxal *vs* glutaraldehyde in biomedical applications," *Environ. Health Persp.* 130(8), article 087009. https://doi.org/10.1289/EHP10985

Setter, C., Zidanes, U. L., de Novais Miranda, E. H., Brito, F. M. S., Mendes, L. M., and Junior, J. B. G. (2021). "Influence of wood species and adhesive type on the performance of multilaminated plywood," *Environ. Sci. Pollut. R.* 28(36), 50835-50846. https://doi.org/10.1007/s11356-021-14283-w

Tene Tayo, L., Shivappa Nayaka, D., Cárdenas-Oscanoa, A. J., and Euring, M. (2025). "Enhancing physical and mechanical properties of single-layer particleboards bonded with canola protein adhesives: Impact of production parameters," *Eur. J. Wood Prod.* 83, article 6. https://doi.org/10.1007/s00107-024-02163-2

Westerman, C. R., McGill, B. C., and Wilker, J. J. (2023). "Sustainably sourced components to generate high-strength adhesives," *Nature* 621, 306-311. https://doi.org/10.1038/s41586-023-06335-7

Wu, L., Gu, W., Li, D., Yang, H., Yang, Q., Li, H., Chen, C., Meng, T., Yang, Y., He, X., *et al.* (2025). "One-step preparation and characterization of a protein–sucrose wood adhesive with excellent bonding performance," *Forests* 16(2), article 318. https://doi.org/10.3390/f16020318

Wu, Z., Liang, J., Lei, H., Zhang, B., Xi, X., and Li, L. (2021). "Study on soy protein-based adhesive cross-linked by glyoxal," *J. Renew. Mater.* 9(2), 205-218. https://doi.org/10.32604/jrm.2021.013655

Wu, Z., Xi, X., Lei, H., and Du, G. (2017). "Soy-based adhesive cross-linked by phenol-formaldehyde-glutaraldehyde," *Polymers* 9(5), article 169. https://doi.org/10.3390/polym9050169

Wu, Z., Xi, X., Lei, H., Liang, J., Liao, J., and Du, G. (2019). "Study on soy-based adhesives enhanced by phenol formaldehyde cross-linker," *Polymers* 11(2), article 365. https://doi.org/10.3390/polym1102036

Xu, G., Zhang, Q., Xi, X., Lei, H., Cao, M., Du, G., and Wu, Z. (2023). "Tannin-based wood adhesive with good water resistance crosslinked by hexanediamine," *Int. J. Biol. Macromol.* 234, article 123644, https://doi.org/10.1016/j.ijbiomac.2023.123644

Xu, Y., Han, Y., Shi, S. Q., Gao, Q., and Li, J. (2020). "Preparation of a moderate viscosity, high performance and adequately-stabilized soy protein-based adhesive *via* recombination of protein molecules," *J. Clean. Prod.* 255, article 120303. https://doi.org/10.1016/j.jclepro.2020.120303

Yamamoto, T., Sato, K., and Nakamura, H. (2020). "Paper wet-strength enhancement using glyoxal: Process optimization and stability assessment," *Ind. Eng. Chem. Res.*

59(45), 19876-19885. https://doi.org/10.1021/acs.iecr.0c03912
Yang, G., Gong, Z., Luo, X., Chen, L., and Shuai, L. (2023). "Bonding wood with uncondensed lignins as adhesives," *Nature* 621, 511-515. https://doi.org/10.1038/s41586-023-06507-5
Yang, I., Kuo, M., and Myers, D. (2006). "Bond quality of soy-based phenolic adhesives in southern pine plywood," *J. Am. Oil Chem. Soc.* 83, 231-237. https://doi.org/10.1007/s11746-006-1198-7
Yao, X., Liu, H., and Li, C. (2025). "Development of eco-friendly soy meal adhesives enhanced by ethylene glycol diglycidyl ether," *Adv. Poly. Tech.* 1, article 8697047. https://doi.org/10.1155/2019/8697047
Zeng, G., Dong, Y., Luo, J., Zhou, Y., Li, C., Li, K., Li, X., and Li, J. (2024). "Desirable strong and tough adhesive inspired by dragonfly wings and plant cell walls," *ACS Nano* 18, 9451-9469. https://doi.org/10.1021/acsnano.3c11160
Zhang, B., Wu, Z., Liang, J., Yu, L., Xi, X., Lei, H., and Du, G. (2022a). "Effects of polyethylene glycol on the flexibility of cold-setting melamine-urea-formaldehyde resin," *Eur. J. Wood Wood Prod.* 80, 975-984. https://doi.org/10.1007/s00107-022-01801-x
Zhang, X., Xu, C., Liu, Z., Shi, S. Q., Li, J., Luo, J., and Gao, Q. (2022b). "A water-resistant and mildewproof soy protein adhesive enhanced by epoxidized xylitol," *Ind. Crop. Prod.* 18, article 114794. https://doi.org/10.1016/j.indcrop.2022.114794
Zheng, L., Li, H., Wang, H., Ruan, R., Li, Z., Tondi, G., Tian, H., and Lei, H. (2025). "Fully biomass-based soybean flour-glucose-citric acid wood adhesive with high strength and water resistance," *Colloid. Surface. A.* 716, article 136664. https://doi.org/10.1016/j.colsurfa.2025.136664
Zhou, Y., Xu, D., Li, C., Pizzi, A., Du, G., and Lei, H. (2025). "Self-neutralizing tannin-citric acid wood adhesives," *Int. J. Biol. Macromol.* 310, article 143419. https://doi.org/10.1016/j.ijbiomac.2025.143419

Article submitted: November 12, 2025; Peer review completed: January 24, 2026;
Revised version received and accepted: March 12, 2026; Published: March 25, 2026.
DOI: 10.15376/biores.21.2.4135-4152